Matters Arising

Neuron

Diversity of Transgenic Mouse Models for Selective Targeting of Midbrain Dopamine Neurons

Highlights

- Low dopamine specificity of transgene expression in ventral midbrain of TH-Cre mice
- DAT-Cre mice exhibit dopamine-specific Cre expression patterns
- VTA GABA and glutamate neurons bi-directionally modulate lateral habenula cells

Authors

Stephan Lammel, Elizabeth E. Steinberg, ..., Liqun Luo, Robert C. Malenka

Correspondence

lammel@berkeley.edu (S.L.), malenka@stanford.edu (R.C.M.)

In Brief

Transgenic Cre-driver mouse lines are an important tool for optogenetic manipulations of neural circuit function. Lammel et al. find that a prominent supposedly dopamine-specific transgenic mouse line exhibits dramatic non-dopamine specific expression patterns in the ventral midbrain.

Lammel et al., 2015, Neuron *85*, 429–438
January 21, 2015
http://dx.doi.org/10.1016/j.neuron.2014.12.036

CellPress

Neuron
Matters Arising

Diversity of Transgenic Mouse Models for Selective Targeting of Midbrain Dopamine Neurons

Stephan Lammel,[1,4,5,*] Elizabeth E. Steinberg,[1,4] Csaba Földy,[1,3,4] Nicholas R. Wall,[1] Kevin Beier,[1,2] Liqun Luo,[2] and Robert C. Malenka[1,*]
[1]Nancy Pritzker Laboratory, Department of Psychiatry and Behavioral Sciences, Stanford University School of Medicine, 265 Campus Drive, Stanford CA 94305-5453, USA
[2]Howard Hughes Medical Institute and Department of Biology, Stanford University, Stanford, CA 94305, USA
[3]Department of Molecular and Cellular Physiology, Stanford University School of Medicine, 265 Campus Drive, Stanford CA 94305-5453, USA
[4]Co-first author
[5]Present address: Department of Molecular and Cell Biology and Helen Wills Neuroscience Institute, University of California Berkeley, 142 Life Sciences Addition #3200, Berkeley CA 94720, USA
*Correspondence: lammel@berkeley.edu (S.L.), malenka@stanford.edu (R.C.M.)
http://dx.doi.org/10.1016/j.neuron.2014.12.036

SUMMARY

Ventral tegmental area (VTA) dopamine (DA) neurons have been implicated in reward, aversion, salience, cognition, and several neuropsychiatric disorders. Optogenetic approaches involving transgenic Cre-driver mouse lines provide powerful tools for dissecting DA-specific functions. However, the emerging complexity of VTA circuits requires Cre-driver mouse lines that restrict transgene expression to a precisely defined cell population. Because of recent work reporting that VTA DA neurons projecting to the lateral habenula release GABA, but not DA, we performed an extensive anatomical, molecular, and functional characterization of prominent DA transgenic mouse driver lines. We find that transgenes under control of the tyrosine hydroxylase, but not the dopamine transporter, promoter exhibit dramatic non-DA cell-specific expression patterns within and around VTA nuclei. Our results demonstrate how Cre expression in unintentionally targeted cells in transgenic mouse lines can confound the interpretation of supposedly cell-type-specific experiments. This Matters Arising paper is in response to Stamatakis et al. (2013), published in *Neuron*. See also the Matters Arising Response paper by Stuber et al. (2015), published concurrently with this Matters Arising in *Neuron*.

INTRODUCTION

Transgenic rodent models that provide genetic access to specific cell populations in the nervous system have become indispensable in modern neuroscience research. In recent years the use of Cre-driver lines in combination with Cre-dependent optogenetic tools has proven to be a particularly fruitful approach, permitting selective, bidirectional control of neural activity in genetically defined cell populations (Deisseroth, 2014; Yizhar et al., 2011). Many of these studies have focused on midbrain dopamine (DA) neurons, thus far identifying roles for these cells in reward, reinforcement, motivation, aversion, depression, social interaction, and other aspects of normal and maladaptive brain function (Chaudhury et al., 2013; Ilango et al., 2014; Lammel et al., 2012; Rothermel et al., 2013; Stamatakis et al., 2013; Steinberg et al., 2013; Tsai et al., 2009; Tye et al., 2013). The most widely implemented approach for targeting midbrain DA neurons involves the use of transgenic Cre-driver mouse lines where Cre recombinase is expressed under the control of tyrosine hydroxylase (TH) or dopamine transporter (DAT) promoters (Lindeberg et al., 2004; Savitt et al., 2005; Zhuang et al., 2005).

In the ventral midbrain, TH, the rate-limiting enzyme in the synthesis of DA, is considered to be the gold standard for identifying DA neurons and is now the most common genetic "handle" used to drive exogenous gene expression. Accordingly, TH-Cre knock-in mouse driver lines have been used in ~80% of the studies that involved Cre-dependent targeting of midbrain DA neurons (Adamantidis et al., 2011; Chaudhury et al., 2013; Chuang et al., 2011; Danjo et al., 2014; Friedman et al., 2014; Gunaydin et al., 2014; Ilango et al., 2014; Kim et al., 2013; Lammel et al., 2012; Rothermel et al., 2013; Stamatakis et al., 2013; Tan et al., 2012; Tsai et al., 2009; Tye et al., 2013; Walsh et al., 2014). Furthermore, the most widely accepted method of confirming DAergic identity in vivo and ex vivo is to demonstrate co-localization of immunohistochemically detected TH with a cell-filling dye injected during recording (Ungless and Grace, 2012).

Using TH-Cre mice, a recent study described a unique population of lateral habenula (LHb)-projecting VTA DA neurons that release GABA but not DA (Stamatakis et al., 2013). Accurate interpretation of these and other experiments that employ cell-type-specific transgenic animals crucially depends on the degree to which transgene expression faithfully reproduces native gene expression patterns. Insofar as Cre expression extends beyond the cellular population of interest, the effects of manipulating unintentionally targeted cells may be erroneously attributed. This issue is especially significant in brain regions where neighboring cells are functionally diverse, such as the

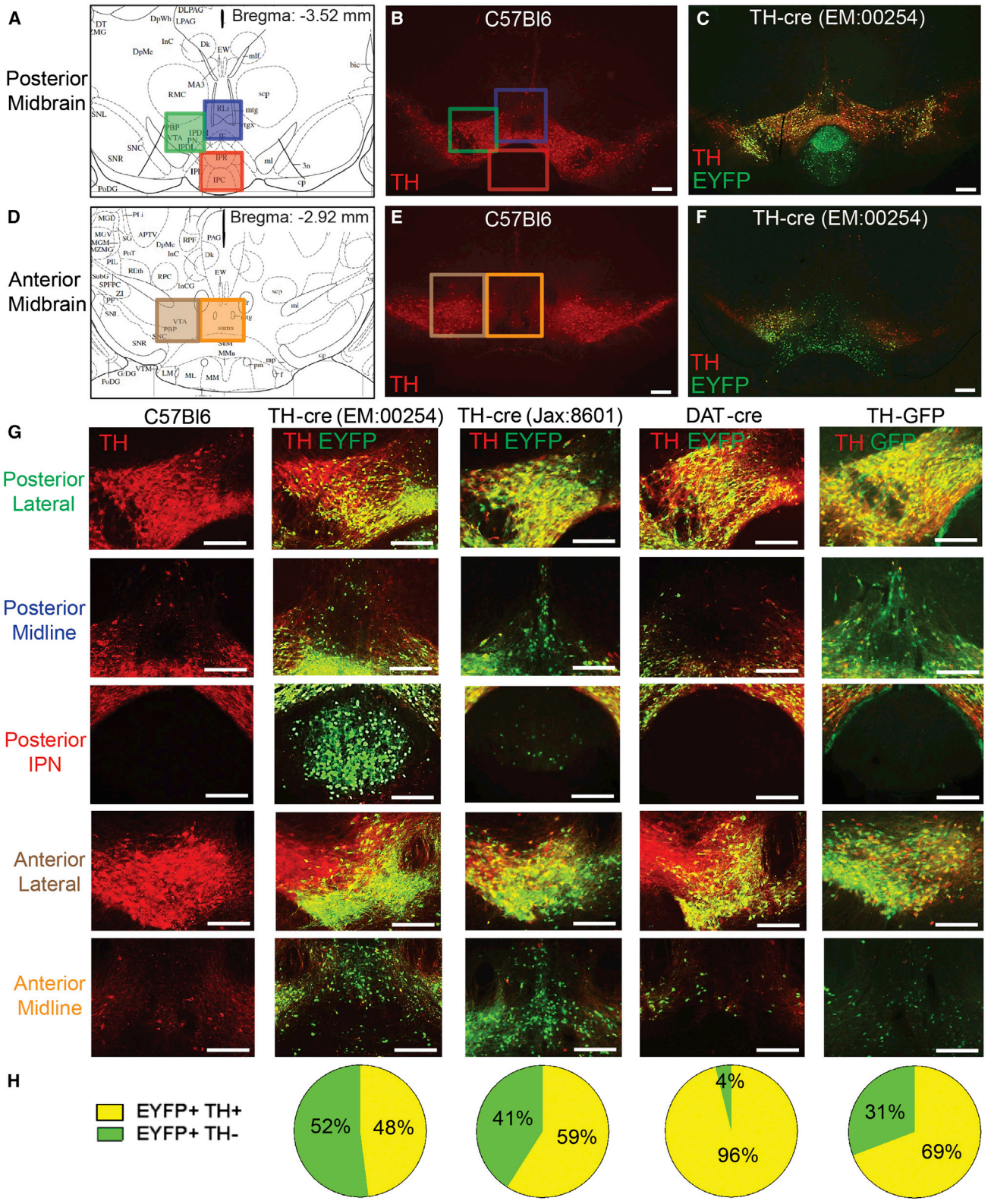

Figure 1. Anatomical Characterization of Transgenic Cre Mouse Driver Lines

(A) Regions of the posterior midbrain in which eYFP/TH co-localization was analyzed (blue: midline VTA; green: lateral VTA, red: interpeduncular nucleus, IPN).

(legend continued on next page)

VTA, which in addition to a heterogeneous population of DA neurons (Fields et al., 2007; Lammel et al., 2014; Roeper, 2013) also contains subpopulations of heterogeneous GABAergic and glutamatergic neurons (Brown et al., 2012; Hnasko et al., 2012; Li et al., 2013; Margolis et al., 2012; Nair-Roberts et al., 2008; Olson and Nestler, 2007). Here, we systematically evaluated prominent DA transgenic mouse lines to assess transgene specificity for midbrain DA neurons. We found that lines employing the TH, but not DAT, promoter exhibit substantial transgene expression in non-DA neurons. By analyzing VTA neurons projecting to LHb in these and other Cre drive mouse lines, we identify a previously unappreciated population of LHb-projecting VTA GABA neurons, thereby highlighting the potential for ectopic expression in supposedly DA-specific mouse lines to cloud our understanding of complex midbrain circuits.

RESULTS

Anatomical Characterization of DA Neuron-Targeted Transgenic Mouse Lines

Double-floxed (DIO) AAV-DJ-eYFP (1 μl, ~10^{12} infectious units/ml) was unilaterally injected into the VTA of TH::IRES-Cre knock-in mice (European Mouse Mutant Archive; stock number: *EM:00254*; backcrossed at least 5 generations with C57Bl/6 mice) (Lindeberg et al., 2004). This injection volume and viral titer is similar to those used by other groups to target midbrain DA neurons with Cre-dependent AAV viruses (Chaudhury et al., 2013; Stamatakis et al., 2013; Tsai et al., 2009; Tye et al., 2013). Surprisingly, TH immunostaining revealed dramatic eYFP expression in TH-immunonegative cells within and adjacent to the VTA, in addition to expression in TH-immunopositive neurons in the VTA and substantia nigra (Figures 1A–1F). Notably, strong eYFP expression was observed in brain areas adjacent to the VTA that typically do not exhibit TH immunostaining, including the interpeduncular nucleus (IPN) and supramammillary (SuM) nucleus. We systematically analyzed co-localization of eYFP expression with immunohistochemically detected TH in five different regions of the posterior (Figures 1A–1C) and anterior (Figures 1D–1F) ventral midbrain. Co-localization was the highest in lateral regions of the posterior and anterior VTA. In contrast, extremely low levels of co-localization were observed in midline VTA regions of the posterior and anterior ventral midbrain. No co-localization was detected in the IPN although we observed strong eYFP expression in this area (Figures 1G and S1A). Importantly, when these five regions were considered collectively, we found similar proportions of eYFP-expressing cells that lacked TH and eYFP-expressing cells that contained TH (eYFP+/TH− 52% ± 3%; eYFP+/TH+ 48% ± 3%; n = 3 mice, Figure 1H).

Given that prior studies that employ TH-Cre mice generally report high levels of TH specificity (> 98%) (e.g., Chaudhury et al., 2013; Stamatakis et al., 2013), we characterized another TH::IRES-Cre knock-in mouse line generated by a different laboratory (Savitt et al., 2005) and obtained from the Jackson Laboratory (stock number: *JAX:8601*). These mice showed a similar eYFP expression pattern (eYFP+/TH− 41% ± 1%; eYFP+/TH+ 59% ± 1%; n = 3 mice, Figures 1G, 1H, and S1B). The high levels of specificity observed in previous studies of TH-Cre mice were likely observed because only lateral portions of the VTA were examined. However, the standard volume of virus we infused (1 μl) spread well beyond the borders of the lateral VTA, making it difficult to envision how optogenetic manipulations could be exclusively confined to this region in order to circumvent the lack of specificity in transgene expression observed in immediately adjacent areas.

Because of the poor specificity of transgene expression in TH-Cre mice, we conducted the same systematic anatomical analysis of transgene expression in DAT-Cre mice (Jackson Laboratory, stock number: 006660) (Zhuang et al., 2005). In marked contrast to TH-Cre mice, TH immunostaining of brain sections from DAT-Cre mice previously injected with AAV-DJ-DIO-eYFP (1 μl) revealed that the overwhelming majority of eYFP-expressing neurons in all ventral midbrain regions were TH-immunopositive (eYFP+/TH− 4% ± 1%; eYFP+/TH+; 96% ± 1%; n = 3 mice, Figures 1G, 1H, and S1C). We also analyzed transgenic mice that expressed GFP under control of the TH promoter (Sawamoto et al., 2001). Co-localization of GFP with TH was similar to that of TH-Cre mice (GFP+/TH− 31% ± 4%; GFP+/TH+ 69% ± 4%; n = 4 mice, Figures 1G, 1H, and S1D).

Additional results suggest that our measures of TH and eYFP/GFP co-localization in TH-driver lines were accurate and not due to leaky expression of Cre-dependent viral constructs, or non-optimal immunohistochemical and/or imaging techniques. First, VTA injection of either AAV5-DIO-eYFP (1 μl) (Figure S1E) or AAV5-DIO-ChR2-eYFP (1 μl, data not shown) shows similar lack of specificity. Second, we observed almost no eYFP expression following double-floxed AAV injections into the VTA of wild-type C57Bl6 mice (< 10 eYFP-positive cells per mouse, n = 2 mice, data not shown). Third, similar expression patterns were observed when we crossed TH-Cre or DAT-Cre mice with a tdTomato reporter line (Ai14). Analysis of co-localization of TH with tdTomato in 3-week-old TH-Cre/Ai14 or DAT-Cre/Ai14 mice revealed substantial expression of tdTomato in TH-immunonegative cells within and adjacent to VTA nuclei in TH-Cre driver lines but not DAT-Cre-driver lines (data not shown). Fourth, DOPA decarboxylase, another key enzyme required for catecholamine synthesis, was also not detectable

(B) Fluorescence image of a coronal brain slice showing TH immunostaining (546 nm, red) of the same region depicted in (A) from a C57Bl6 mouse. Note the low number of TH-immunopositive cells in the midline VTA region (blue) and absence of TH-positive cells in the IPN (red).
(C) Fluorescence image showing eYFP expression (488 nm, green) and TH immunostaining (546 nm, red) of the same region depicted in (A) from a TH-Cre mouse.
(D) Mouse brain atlas showing areas in the anterior midbrain in which eYFP/TH co-localization has been analyzed (brown: lateral VTA; orange: midline VTA).
(E) Fluorescence image of a coronal brain slice showing TH immunostaining (546 nm, red) of the same region depicted in (D) from a C57Bl6 mouse. Note the very low number of TH-immunopositive cells in the midline VTA region (orange).
(F) Fluorescence image showing eYFP-expression (488 nm, green) and TH immunostaining (546 nm, red) of the same region depicted in (D) from a TH-Cre mouse.
(G) Fluorescence images comparing the areas depicted in (A) and (D) for different transgenic mouse driver lines (eYFP, 488 nm, green; TH, 546 nm, red).
(H) Pie charts showing the total percentage of co-localization of eYFP with TH-immunopositive (yellow) or TH-immunonegative (green) cells for the five color-coded areas depicted in (A) and (D) and for the mouse lines presented in (G). All scale bars: 200 μm.

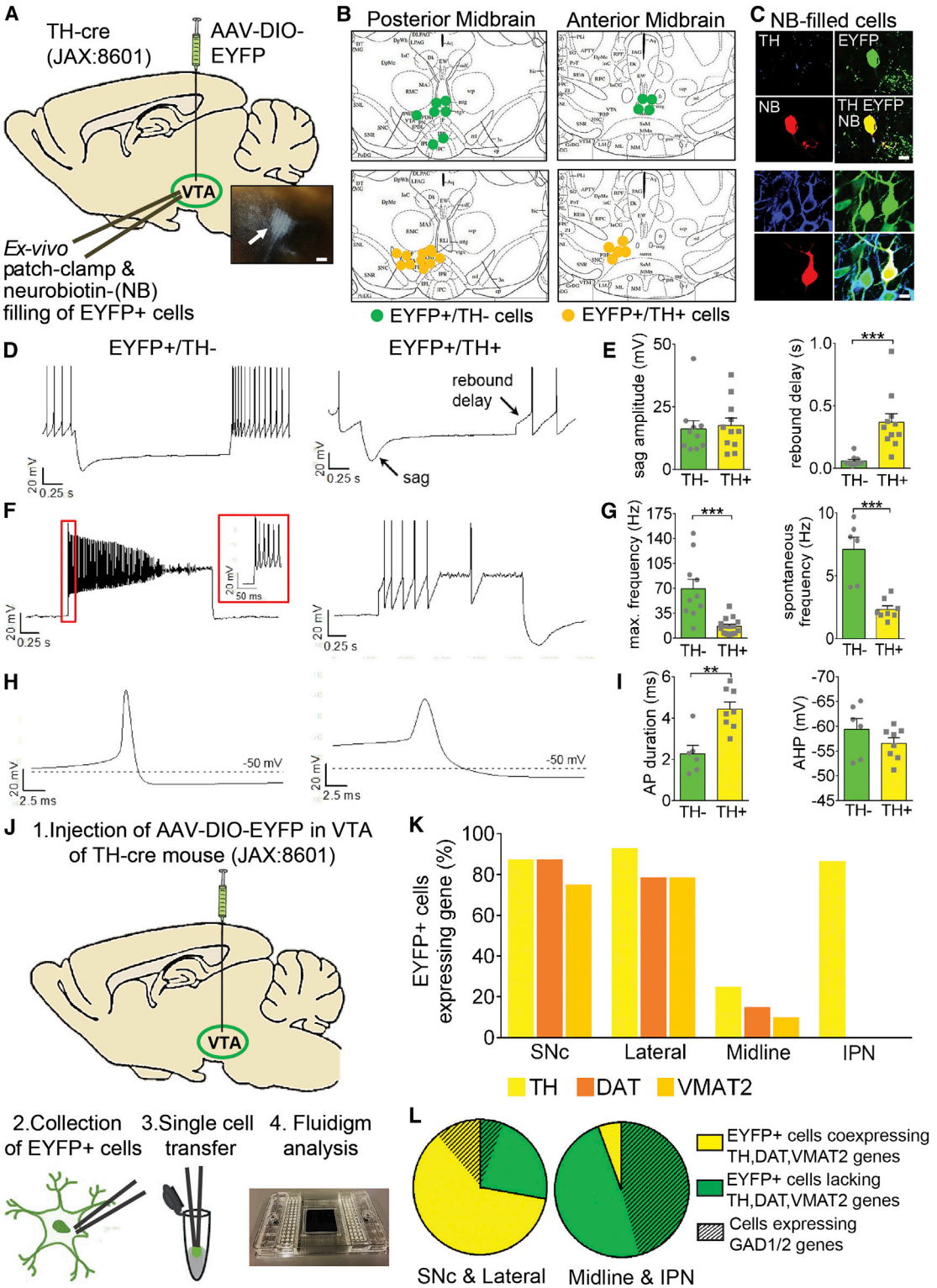

Figure 2. Electrophysiological and Molecular Properties of eYFP-Expressing Cells in TH-Cre Mice

(A) Experimental approach for characterizing electrophysiological properties of eYFP-expressing cells in TH-Cre mice. Inset shows a neuron expressing eYFP prior to recording. Scale bar: 10 μm.

(B) Anatomical positions of the recorded and neurobiotin-filled cells that are TH immunonegative (green) or TH immunopositive (yellow).

(legend continued on next page)

in eYFP+/TH− cells (Figure S2A). Fifth, in TH-Cre mice that received VTA-targeted injections of AAV-DJ-DIO-eYFP we observed substantial axonal eYFP expression in brain regions (LHb and lateral septum) with extremely low TH immunoreactivity. This pattern was not observed in DAT-Cre mice (Figures S2B and S2C). Sixth, we tested two different TH antibodies (Calbiochem and Pel-Freez), but neither led to detectable cellular TH immunosignals in areas such as the IPN or SuM, which would explain the transgene expression patterns observed in TH-Cre mice (data not shown).

Different Electrophysiological and Molecular Properties of Cre-Expressing DA and Non-DA Neurons

Because many midbrain cells in TH-Cre mice expressed eYFP but did not show TH immunostaining, we next determined whether the electrophysiological properties of eYFP+/TH− cells were distinct from those of eYFP+/TH+ cells. To accomplish this, we injected AAV-DJ-DIO-eYFP (1 μl) into the VTA of TH-Cre mice (*JAX:8601)* and performed whole-cell recordings from eYFP-positive neurons in coronal midbrain slices (Figure 2A). Cells were filled with neurobiotin during recordings and subsequently analyzed for neurochemical phenotype using TH immunohistochemistry. Consistent with our anatomical characterization, we found eYFP+/TH− cells in midline VTA regions of the posterior and anterior midbrain as well as in the IPN. In contrast, most eYFP-expressing cells in more lateral VTA regions were TH+ (Figures 2B and 2C).

Upon injection of hyperpolarizing currents both eYFP+/TH+ and eYFP+/TH− cells showed large variability in the amplitude of the sag component that is mediated by HCN (hyperpolarization-activated cyclic nucleotide-gated) channels (sag amplitude: TH−, 16.2 ± 3.4 mV, n = 10; TH+, 17.5 ± 3 mV, n = 11; p = 0.7656) (Figures 2D and 2E). However, upon repolarization at the end of the hyperpolarizing step, eYFP+/TH+ cells showed a prominent inhibition of spike firing with a slow return to the firing threshold. In contrast, lack of a prominent rebound delay was nearly uniform in eYFP+/TH− cells (TH−, 58.5 ± 12.6 ms, n = 10; TH+, 368.4 ± 68.3 ms, n = 10; p = 0.0004) (Figures 2D and 2E). In addition, the maximal firing frequencies in response to increasing steps of current injections (TH−, 69.3 ± 13.6 Hz, n = 10; TH+, 16.8 ± 2.9 Hz, n = 15; p = 0.0001) (Figures 2F and 2G) as well as the spontaneous discharge rate (TH−, 7.1 ± 1 Hz, n = 6; TH+, 2.3 ± 0.3, n = 8; p = 0.0002) (Figure 2G) were in most cases higher in eYFP+/TH− cells as compared to eYFP+/TH+ cells. Analysis of fully resolved action potentials (AP) revealed that AP durations in eYFP+/TH− cells were in most cases shorter than those of eYFP+/TH+ cells (Figures 2H and 2I) (AP duration at threshold: TH−, 2.3 ± 0.4 ms, n = 6; TH+, 4.4 ± 0.3 ms, n = 8; p = 0.0016). There were no significant differences in the single AP afterhyperpolarization (AHP: TH−, −59.4 ± 2.2 mV, n = 6; TH+, −56.5 ± 1.1 mV, n = 8; p = 0.2342) (Figure 2I) nor AP threshold (data not shown). Importantly, the electrophysiological properties of eYFP+/TH− cells are consistent with properties previously observed in VTA GABAergic neurons (Chieng et al., 2011; Johnson and North, 1992; Korotkova et al., 2004), and are substantially different from identified DA subpopulations, including those with unconventional electrophysiological properties (e.g., mesocortical DA neurons, see Lammel et al., 2008).

We next quantified the gene expression profiles of single eYFP+ neurons in TH-Cre knock in mice (*JAX:8601)* by extracting their intracellular contents and using parallel quantitative real-time PCR (Fluidigm, BioMark) (Figure 2J). Most eYFP+ cells in the substantia nigra pars compacta (SNc) and lateral VTA expressed genes classically associated with DA synthesis (TH: tyrosine hydroxylase), uptake (DAT: dopamine transporter), and release (VMAT2: vesicular monamine transporter 2) (SNc TH: 87.5%, DAT: 87.5%, VMAT2: 75%, n = 8; lateral VTA TH: 92.9%, DAT: 78.6%, VMAT2: 78.6%, n = 28). In contrast, in midline VTA regions a much smaller percentage of eYFP+ cells expressed these genes (TH: 25%, DAT: 15%, VMAT2: 10%, n = 20). Even though eYFP+ cells in the IPN did not express detectable TH protein, the vast majority of these cells did exhibit detectable levels of TH mRNA transcipts. However, these cells completely lacked other important DAergic marker genes such as DAT and VMAT2 (TH: 86.7%, DAT: 0%, VMAT2: 0%, n = 15) (Figures 2K and S3). Furthermore, while ~75% of eYFP+ neurons in the SNc and lateral VTA co-expressed TH, DAT, and VMAT2 (72.2%, n = 26/36 cells), only ~6% of the cells in IPN and midline VTA regions co-expressed these genes (5.7%,

(C) Sample confocal images of individual eYFP-expressing cells (488 nm, green) that were filled with neurobiotin (NB; 546 nm, red) via the recording pipette and immunostained for tyrosine-hydroxylase (TH; 647 nm, blue). All scale bars: 10 μm.

(D) Sample whole-cell patch-clamp recording from an eYFP-expressing cell that has been NB-filled and posthoc stained for TH. Left: TH-immunonegative cell; right: TH-immunopositive cell. Corresponding membrane potentials in response to hyperpolarizing currents shows lack of rebound delay in TH-immunonegative cells. Note that both cell types show prominent sags during the hyperpolarizing steps.

(E) Bar graphs showing mean sag amplitudes (left) and mean rebound delays (right) for eYFP+/TH− (green) and eYFP+/TH+ (yellow) cells. ***p < 0.001. Data represent means ± SEM.

(F) Corresponding membrane-potential responses to depolarizing current pulses. Note that eYFP+/TH− (left) and eYFP+/TH+ (right) cells show depolarization block of spontaneous electrical activity after discharging at different maximal frequencies.

(G) Bar graphs showing mean maximal firing frequency after reaching depolarizing block (left) and mean spontaneous firing frequencies (no current injections) from eYFP+/TH− (green) and eYFP+/TH+ (yellow) cells. ***p < 0.001. Data represent means ± SEM.

(H) Single high-resolution action-potential (AP) waveforms from an eYFP+/TH− (left) or eYFP+/TH+ (right) cell.

(I) Bar graphs showing mean AP duration (left) and mean afterhyperpolarization (AHP) amplitudes (right) for eYFP+/TH− (green) and eYFP+/TH+ (yellow) cells. **p < 0.01. Data represent means ± SEM.

(J) Schematic drawing of the experimental approach to analyze gene expression profiles of eYFP-expressing cells in TH-Cre mice.

(K) Bar graph comparing the percentage of eYFP-expressing cells that express TH, DAT, or VMAT2 genes in the substantia nigra pars compacta (SNc), lateral VTA, midline VTA, and interpeduncular nucleus (IPN).

(L) Pie charts showing eYFP-expressing cells that co-express TH, DAT, and VMAT2 (yellow) or lack co-expression of TH, DAT, and VMAT2 (green) for SNc and lateral VTA as well as midline VTA and IPN regions. Striped area indicates cells expressing GAD1 and/or GAD2 genes.

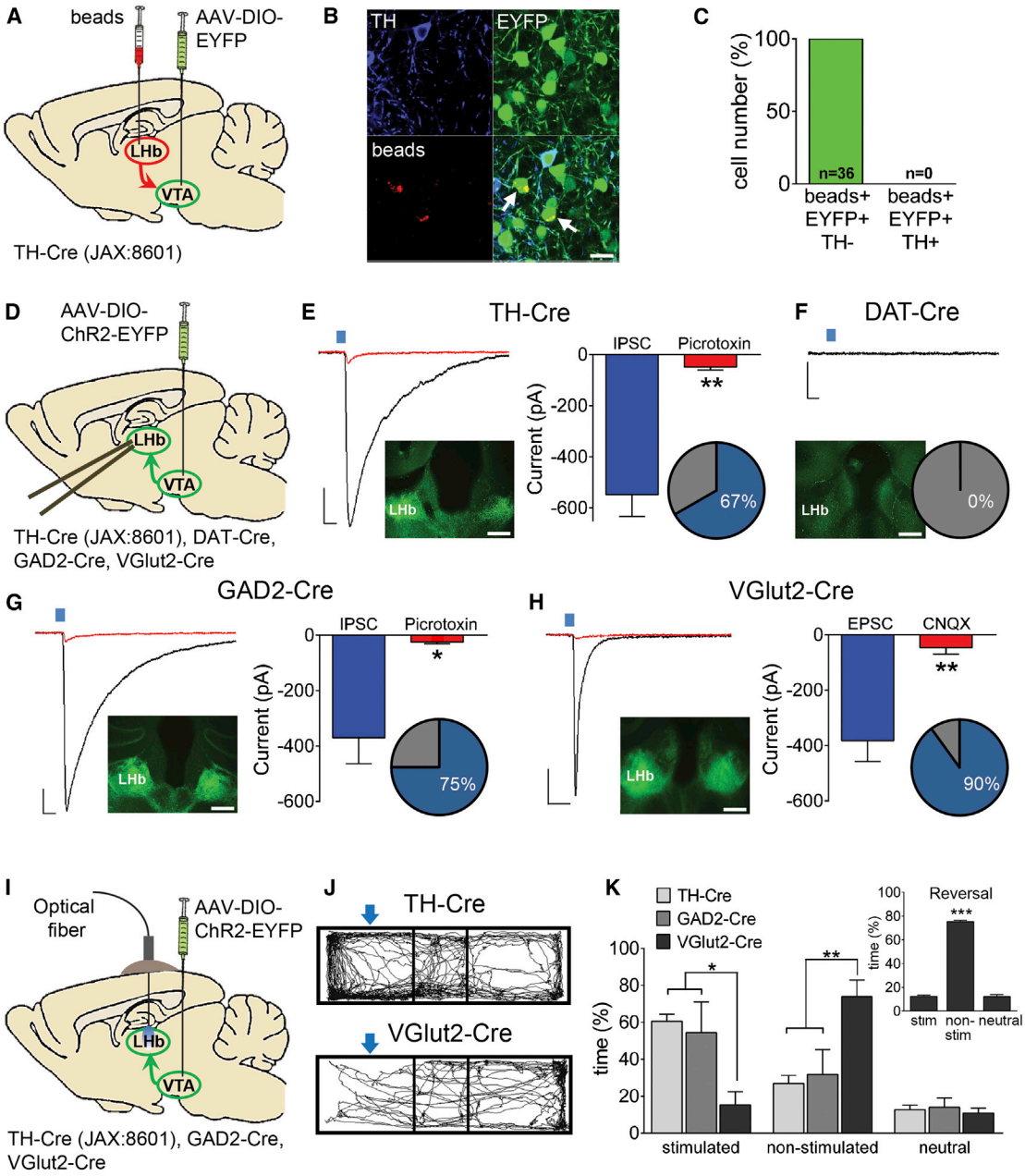

Figure 3. Optogenetic Dissection of the Mesohabenular Pathway

(A) Schematic showing dual injections of fluorescent beads into the LHb and AAV into the VTA of a TH-Cre mouse (*JAX:8601*).

(B) Confocal image demonstrating retrogradely labeled (i.e., bead-containing, 546 nm, red) and TH (647 nm, blue)-immunonegative VTA neurons that express eYFP (488 nm, green). Scale bar: 20 μm.

(C) Bar graph showing that all retrogradely labeled cells that also express eYFP do not possess detectable TH immunosignals.

(D) Schematic of AAV injection into the VTA of TH-Cre, DAT-Cre, GAD2-Cre, and VGlut2-Cre mice and ex vivo whole-cell patch-clamp recordings of LHb neurons.

(E) Left: light-evoked IPSCs recorded from LHb neurons in TH-Cre mice are blocked by bath application of picrotoxin (red trace). Scale bar: 100 pA, 10 ms. Inset shows ChR2-eYFP (488 nm, green) expression in the LHb of a TH-Cre mouse. Scale bar: 200 μm. Right: bar graph showing mean IPSC amplitudes before (blue) and after (red) bath application of picrotoxin. Pie chart indicates the percentage of recorded LHb neurons that responded to light stimulation. $^{**}p < 0.01$. Data represent means ± SEM.

(F) Same experimental approach as in Figure 3E, but for DAT-Cre mice.

(G) Same experimental approach as in Figure 3E, but for GAD2-Cre mice. $^{*}p < 0.05$. Data represent means ± SEM.

(H) Left: light-evoked EPSCs recorded from LHb neurons in VGlut2-Cre mice are blocked by bath application of CNQX (red trace). Scale bar: 100 pA, 10 ms. Inset shows ChR2-eYFP (488 nm, green) expression in the LHb of a VGlut2-Cre mouse. Scale bar: 200 μm. Right: bar graph showing mean EPSC amplitudes before

(legend continued on next page)

n = 2/35 cells). In contrast, nearly half of the eYFP+ cells in the IPN and midline VTA that lacked co-expression of TH, DAT, and VMAT2 showed detectable levels of GAD1/2 gene expression (48.6%, n = 17/35 cells). Only ~6% of the eYFP+ cells that co-expressed TH, DAT, and VMAT2 expressed GAD1/2 (5.6%, n = 2/36) (Figures 2L and S3).

Optogenetic Dissection of the Mesohabenular Pathway using Transgenic Mouse Lines

TH-Cre mice that received VTA-targeted injections of AAV-DJ-DIO-eYFP showed substantial axonal eYFP expression in the LHb while TH-immunolabeled terminals are almost completely absent (Figure S2B; Hnasko et al., 2012; Stamatakis et al., 2013). Because of this inconsistency the existence of a unique population of VTA DA neurons that projects to the LHb has been proposed. Specifically, using TH-Cre knock-in mice (TH::IRES-Cre) it was demonstrated that optogenetic activation of this projection inhibits LHb neurons via synaptically released GABA, but not DA, to promote reward-related behaviors (Stamatakis et al., 2013). Because of the prominent ectopic patterns of transgene expression we observed in TH-Cre mice we re-evaluated this conclusion by first injecting retrobeads into the LHb and AAV-DJ-DIO-eYFP (1 μl) into the VTA of TH-Cre mice (*JAX:8601*). Consistent with previous reports (Gruber et al., 2007; Skagerberg et al., 1984; Stamatakis et al., 2013; Swanson, 1982), retrogradely labeled neurons were predominately located in midline VTA nuclei of the anterior and posterior midbrain. However, all retrogradely labeled cells that expressed eYFP were also TH-immunonegative (n = 36/36 cells, n = 2 mice) (Figures 3A–3C). Indeed, additional retrograde tracing experiments in C57Bl6 wild-type mice revealed that the vast majority (~97%–99%) of the mesohabenular neurons were TH-immunonegative (Figures S4A–S4H). To determine the neurochemical phenotype of VTA neurons projecting to LHb we injected retrobeads into the LHb of GAD2-Cre and VGlut2-Cre mice that had been crossed with an Ai14 reporter line. Virtually all of the LHb-projecting, retrobead-containing cells expressed GABAergic or glutamatergic markers with few if any TH-immunopositive neurons (Figures S4I and S4J). Importantly, a recent study suggests that the majority of mesohabenular neurons co-express both GABAergic and glutamatergic molecular markers, but do not possess detectable TH immunosignals (Root et al., 2014a).

To further dissect the functional role of mesohabenular projections, we injected AAV5-DIO-ChR2-eYFP (1 μl) into the VTA of TH-Cre (*JAX:8601*), DAT-Cre, GAD2-Cre, and VGlut2-Cre mice (Figure 3D). We observed strong ChR2 expression in the LHb of all transgenic lines except DAT-Cre mice, which showed extremely sparse ChR2 expression within the LHb (Figures 3E–3H; Figure S2B). Voltage clamp recordings from LHb neurons revealed that light pulses that selectively stimulated TH-Cre or GAD2-Cre ChR2 fibers in the LHb evoked inhibitory postsynaptic currents (IPSCs) that were almost completely blocked by the GABA-A receptor antagonist picrotoxin (50 μM) (TH-Cre: −548.2 ± 85.8 pA, n = 8, in picrotoxin: −48.9 ± 12 pA, n = 4, p = 0.0025; GAD2-Cre: −370.4 ± 94.1 pA, n = 9, in picrotoxin: −25.3 ± 5.6 pA, n = 5, p = 0.02). Of the neurons recorded in the LHb ~67% (n = 8/12 cells) received direct monosynaptic inhibitory input from VTA TH-Cre neurons and 75% (n = 9/12 cells) received direct monosynaptic inhibitory input from VTA GAD2-Cre neurons (Figures 3E and 3G). Light pulses never evoked detectable IPSCs in LHb neurons from DAT-Cre mice (n = 0/15 cells) (Figure 3F). In contrast, light stimulation of VGlut2-Cre ChR2 fibers in the LHb evoked excitatory postsynaptic currents (EPSCs) that were blocked by an AMPA (α-amino-3-hydroxy-5-methyl-4-isoxazole propionic acid) receptor antagonist (−382.6 ± 75.8 pA, n = 9, in 10 μM CNQX: −46.6 ± 23.1 pA, n = 7, p = 0.002) in 90% (n = 9/10 cells) of LHb neurons, thus revealing a strong direct excitatory input from VTA VGlut2-Cre neurons to LHb (Figure 3H).

Optogenetic activation of the mesohabenular pathway in TH-Cre mice induced a reward-related phenotype that required GABA release in the LHb (Stamatakis et al., 2013). Our results suggest that we should observe a similar behavioral phenotype in both TH-Cre and GAD2-Cre mice. In contrast, as optogenetic activation of excitatory inputs from the entopeduncular nucleus to LHb as well as from LHb to RMTg/VTA mediates aversive behaviors (Lammel et al., 2012; Shabel et al., 2012; Stamatakis and Stuber, 2012), we hypothized that activation of excitatory mesohabenula projections in the LHb of VGlut2-Cre mice would generate aversion. These predictions were confirmed using a real-time place preference assay in TH-Cre (*JAX:8601*) (n = 4), GAD2-Cre (n = 5), and VGlut2-Cre (n = 4) mice that were injected in the VTA with AAV5-DIO-ChR2-eYFP (1 μl) and implanted with bilateral optical fibers above the LHb (Figures 3I–3K). Activation of mesohabenula projections in the LHb of VGlut2-Cre mice caused a robust real-time place aversion (stimulation compartment versus non-stimulation compartment p = 0.003; 2-way repeated-measures ANOVA followed by Student-Newman-Keuls post hoc test; Figure 3J lower panel, and Figure 3K). Indeed, switching the stimulation to the original non-stimulated compartment caused immediate avoidance of that compartment (p < 0.001; Figure 3K inset). In contrast, consistent with previous work (Stamatakis et al., 2013), activation of mesohabenula projections in the LHb of TH-Cre mice and GAD2-Cre mice

(blue) and after (red) bath application of CNQX. Pie chart indicates the percentage of recorded LHb neurons that responded to light stimulation. **p < 0.01. Data represent means ± SEM.

(I) Schematic of AAV injection into the VTA of TH-Cre, GAD2-Cre, and VGlut2-Cre mice and light activation of LHb terminals.

(J) Location of a TH-Cre (upper panel) and a VGlut2-Cre (lower panel) animal that received stimulation in the compartment marked by the blue arrow.

(K) TH-Cre (n = 4) and GAD2-Cre (n = 5) mice show a mild preference for the compartment paired with optical stimulation, while VGlut2-Cre mice (n = 4) robustly avoid the same compartment. A 2-way repeated-measures ANOVA revealed a main effect of compartment ($F_{2,20}$ = 7.171, p = 0.004) and a genotype × compartment interaction ($F_{4,20}$ = 4.448, p = 0.01). Student-Newman-Keuls post-hoc tests demonstrated that TH-Cre and GAD2-Cre mice did not differ from each other in the amount of time spent in stimulated or non-stimulated compartments (p values > 0.63), but both differed from VGlut2-Cre mice on the same measures (p values < 0.012). Inset graph shows that reversing the compartment in which VGlut2-Cre animals received stimulation caused robust avoidance of that compartment. Data represent means ± SEM, *p < 0.05, **p < 0.01.

caused a more modest rewarding behavioral response. Both groups spent more time in the compartment where they received stimulation as compared to the compartment where they did not receive stimulation (Figure 3J upper panel, and Figure 3K; although this comparison did not reach statistical significance; $p = 0.061$ for TH-Cre, $p = 0.158$ for GAD2-Cre). Furthermore, TH-Cre and GAD2-Cre mice spent more time in the compartment where they received stimulation compared to the neutral area in our three-chamber assay (p values < 0.041) whereas there was no significant difference between time spent in the non-stimulated compartment versus the neutral area (p values > 0.255). Importantly, the behaviors of the the TH-Cre and GAD2-Cre mice did not differ from each other yet both dramatically differed from the VGlut2-Cre mice (Figure 3K; VGlut2-Cre versus TH-Cre/GAD2-Cre all p values < 0.012 for stimulation/non-stimulation compartments; TH-Cre versus GAD2-Cre all p values > 0.63 on the same measures).

DISCUSSION

We have performed an extensive anatomical, molecular, and functional characterization of transgenic mouse lines commonly used to identify and target midbrain DA neurons (TH-Cre, DAT-Cre and TH-GFP mice) and found that TH-Cre knock-in mouse lines exhibit pronounced transgene expression in non-DAergic, i.e., TH-immunonegative, neurons in the VTA and adjacent nuclei. Previous studies have shown that the expression levels of DA-related genes such as TH, DAT, and VMAT2 vary among VTA DA neurons with DA neurons in medial regions of the VTA tending to express lower levels of TH and DAT (Lammel et al., 2008; Li et al., 2013). If TH protein or mRNA was present but levels fell below our threshold for detection in TH driver lines, this could theoretically account for the reduced fidelity we observed in midline regions. However, these unconventional DA neurons (e.g., mesocortical DA neurons) possess detectable TH immunosignals as well as other key enzymes in the synthesis of catecholamines such as DDC (Lammel et al., 2008), markers that were completely absent in many eYFP+ neurons in this study. Furthermore, the ectopic expression observed in TH-Cre mice extends well beyond typical VTA regions and can be found in areas that either are not known to contain DA neurons (e.g., IPN, supramamillary nucleus) or contain only a few scattered DA neurons (e.g., area between the fasciculus retroflexus in the anterior midbrain). Indeed, transgene-expressing cells in these regions expressed neither detectable TH nor DDC immunosignals. Moreover, our single-cell profiling data show that nearly half of the Cre-expressing cells in the IPN and midline VTA nuclei possess GAD1/2 genes but lack co-expression of DA markers including TH, DAT, and VMAT2. This is consistent with previous studies indicating that GABAergic neurons are particularly prominent in these regions (Nair-Roberts et al., 2008; Olson and Nestler, 2007). These cells also lacked a rebound delay in spiking following a prolonged hyperpolarization and fired at higher frequencies, properties typically found in VTA GABAergic neurons but not in identified DA subpopulations (Chieng et al., 2011; Johnson and North, 1992; Korotkova et al., 2004; Li et al., 2012; Lammel et al., 2008).

Because the ability to selectively target DA neurons is critical for the meaningful interpretation of "DA-specific" experiments, we also demonstrate how this ectopic expression can confound data interpretation by focusing on the identity and function of projections from the VTA to the LHb, which has a central role in the control of motivated behaviors via its reciprocal projections to the VTA and the adjacent rostromedial tegmental nucleus (Bromberg-Martin et al., 2010; Hikosaka, 2010; Hong et al., 2011; Lammel et al., 2012; Meye et al., 2013; Stamatakis and Stuber, 2012). Our results demonstrate that < 2% of murine mesohabenular projections arise from DA (i.e., TH-immunopositive) neurons, which may explain the absence of TH-immunolabeled axons in the LHb in mice (Figure S2B) (Hnasko et al., 2012; Stamatakis et al., 2013), the lack of detectable DA release in the LHb of mice (Stamatakis et al., 2013), and that transmitter release in the LHb is not affected by VMAT2-inhibition (Stamatakis et al., 2013). Although in rats the number of VTA DA neurons projecting to LHb seems to be higher (Root et al., 2014a; Gruber et al., 2007; Skagerberg et al., 1984) and terminals expressing both TH as well as functional D2 and D4 receptors have been reported (Good et al., 2013; Jhou et al., 2013; Gruber et al., 2007), it appears that in both species the majority of mesohabenular neurons signal through GABA and/or glutamate (Figures S4I and S4J) (Root et al., 2014a).

Furthermore, we present several lines of evidence that the LHb-projecting VTA neurons that release GABA should not be considered dopaminergic. First, both the majority of transgene-expressing TH- and DDC-immunonegative cells in TH-Cre mice and TH-immunonegative cells projecting to LHb are located in the same VTA region (Figures 1 and S4). Second, in TH-Cre mice, eYFP+ neurons projecting to LHb do not express detectable TH immunosignals (Figures 3A–3C). Third, in TH-Cre mice, eYFP+/TH− cells possess molecular and electrophysiological properties that are characteristic of VTA GABA neurons (Figure 2). Fourth, robust light-evoked IPSCs in LHb neurons were generated in both TH-Cre and GAD2-Cre mice but not DAT-Cre mice when VTA projections were optogenetically activated (Figures 3E–3G). Fifth, in vivo optogenetic activation of VTA projections in the LHb induces a similar behavioral phenotype in both TH-Cre and GAD2-Cre mice (Figure 3K). In addition, consistent with a recent study (Root et al., 2014b) and single-unit recording data reporting that absence of a reward or punishment excites LHb neurons (Hikosaka, 2010; Matsumoto and Hikosaka, 2007, 2009), we also identified a novel role for LHb-projecting VTA glutamate neurons in promoting aversion.

Ectopic expression driven by the TH promoter has been described previously (Lindeberg et al., 2004; Min et al., 1994; Savitt et al., 2005), possibly as a result of inappropriate expression driven by an exogenous promoter, or because of TH promoter activity in precursor cell populations that either never produced TH protein or subsequently lost this ability, potentially as a consequence of post-transcriptional regulation of TH mRNA (Lindeberg et al., 2004). Although we found widespread ectopic transgene expression in TH-Cre mice, virtually all studies that involve optogenetic manipulation of DA neurons in these lines consistently report the presence of TH protein in more than 98% of Cre-expressing cells in midbrain VTA nuclei (e.g., Chaudhury et al., 2013; Ilango et al., 2014; Stamatakis et al., 2013; Tsai et al.,

2009). This likely occurred because lateral regions of the VTA were considered in isolation (Figure S1). Using common optogenetic experimental configurations, it also seems likely that the inherent difficulty in restricting the spread of viral infection and the light path to a precisely circumscribed area will lead to manipulation of non-DA neurons concurrently with targeted DA neurons. Studies that seek to selectively visualize or manipulate axonal projections of DA neurons in TH-Cre driver lines present a related problem, as the location of the corresponding somata is often not identified and projections of interest may in fact derive from neurons with ectopic transgene expression. Although DAT-Cre mice are likely to suffer from their own limitations (for example, low DAT expression in mesocortical DA neurons may make it difficult to target this subpopulation, see Lammel et al., 2008), our results suggest that transgene expression is much more specific in this line. Regardless of the mouse line chosen, validating key assumptions and conclusions with complementary methodologies—such as pharmacological maniulations, careful immunohistochemical studies, or mRNA read-outs—will considerably strengthen conclusions drawn from the use of transgenic mouse lines, which certainly will continue to be a critically important tool for cell-type-specific analyses and manipulations in the mammalian brain.

EXPERIMENTAL PROCEDURES

Immunohistochemistry, Optogenetics, and recordings from VTA neurons were performed essentially as previously described (Lammel et al., 2008, 2011, 2012). All experimental procedures are described in detail in Supplemental Information.

SUPPLEMENTAL INFORMATION

Supplemental Information includes four figures and Supplemental Experimental Procedures and can be found with this article online at http://dx.doi.org/10.1016/j.neuron.2014.12.036.

AUTHOR CONTRIBUTIONS

S.L., E.S., and C.F. contributed equally to performing the experiments in this study. Stereotactic injections were performed by S.L. and E.S. Immunohistochemistry was performed by S.L., E.S., N.W., and K.B. Electrophysiology was performed by S.L. and C.F. Single-cell mRNA profiling was performed by C.F. Behavior experiments were performed by E.S. and S.L. The study was designed by S.L. and R.C.M. Results were analyzed and interpreted by S.L., E.S. and R.C.M with assistance of the other authors. The manuscript was written by S.L., E.S., and R.C.M. and edited by all authors.

ACKNOWLEDGMENTS

We thank the Stanford Neuroscience Imaging Core and the Stanford Neuroscience Gene Vector and Virus Core (all supported by National Institutes of Health grant NIH NS069375). We thank Alexander Nectow (Rockefeller University) for providing TH immunohistochemistry using the Pel-Freez TH antibody. This work was supported by grants from NIDA (K99DA034029 to C.F; DA008227 to R.C.M.), NIMH (TR01-MH099647 to L.L.), and SFARI (R.C.M.).

Accepted: December 16, 2014
Published: January 21, 2015

REFERENCES

Adamantidis, A.R., Tsai, H.C., Boutrel, B., Zhang, F., Stuber, G.D., Budygin, E.A., Touriño, C., Bonci, A., Deisseroth, K., and de Lecea, L. (2011). Optogenetic interrogation of dopaminergic modulation of the multiple phases of reward-seeking behavior. J. Neurosci. *31*, 10829–10835.

Bromberg-Martin, E.S., Matsumoto, M., and Hikosaka, O. (2010). Dopamine in motivational control: rewarding, aversive, and alerting. Neuron *68*, 815–834.

Brown, M.T.C., Tan, K.R., O'Connor, E.C., Nikonenko, I., Muller, D., and Lüscher, C. (2012). Ventral tegmental area GABA projections pause accumbal cholinergic interneurons to enhance associative learning. Nature *492*, 452–456.

Chaudhury, D., Walsh, J.J., Friedman, A.K., Juarez, B., Ku, S.M., Koo, J.W., Ferguson, D., Tsai, H.-C., Pomeranz, L., Christoffel, D.J., et al. (2013). Rapid regulation of depression-related behaviours by control of midbrain dopamine neurons. Nature *493*, 532–536.

Chieng, B., Azriel, Y., Mohammadi, S., and Christie, M.J. (2011). Distinct cellular properties of identified dopaminergic and GABAergic neurons in the mouse ventral tegmental area. J. Physiol. *589*, 3775–3787.

Chuang, J.-C., Perello, M., Sakata, I., Osborne-Lawrence, S., Savitt, J.M., Lutter, M., and Zigman, J.M. (2011). Ghrelin mediates stress-induced food-reward behavior in mice. J. Clin. Invest. *121*, 2684–2692.

Danjo, T., Yoshimi, K., Funabiki, K., Yawata, S., and Nakanishi, S. (2014). Aversive behavior induced by optogenetic inactivation of ventral tegmental area dopamine neurons is mediated by dopamine D2 receptors in the nucleus accumbens. Proc. Natl. Acad. Sci. USA *111*, 6455–6460.

Deisseroth, K. (2014). Circuit dynamics of adaptive and maladaptive behaviour. Nature *505*, 309–317.

Fields, H.L., Hjelmstad, G.O., Margolis, E.B., and Nicola, S.M. (2007). Ventral tegmental area neurons in learned appetitive behavior and positive reinforcement. Annu. Rev. Neurosci. *30*, 289–316.

Friedman, A.K., Walsh, J.J., Juarez, B., Ku, S.M., Chaudhury, D., Wang, J., Li, X., Dietz, D.M., Pan, N., Vialou, V.F., et al. (2014). Enhancing depression mechanisms in midbrain dopamine neurons achieves homeostatic resilience. Science *344*, 313–319.

Good, C.H., Wang, H., Chen, Y.-H., Mejias-Aponte, C.A., Hoffman, A.F., and Lupica, C.R. (2013). Dopamine D4 receptor excitation of lateral habenula neurons via multiple cellular mechanisms. J. Neurosci. *33*, 16853–16864.

Gruber, C., Kahl, A., Lebenheim, L., Kowski, A., Dittgen, A., and Veh, R.W. (2007). Dopaminergic projections from the VTA substantially contribute to the mesohabenular pathway in the rat. Neurosci. Lett. *427*, 165–170.

Gunaydin, L.A., Grosenick, L., Finkelstein, J.C., Kauvar, I.V., Fenno, L.E., Adhikari, A., Lammel, S., Mirzabekov, J.J., Airan, R.D., Zalocusky, K.A., et al. (2014). Natural neural projection dynamics underlying social behavior. Cell *157*, 1535–1551.

Hikosaka, O. (2010). The habenula: from stress evasion to value-based decision-making. Nat. Rev. Neurosci. *11*, 503–513.

Hnasko, T.S., Hjelmstad, G.O., Fields, H.L., and Edwards, R.H. (2012). Ventral tegmental area glutamate neurons: electrophysiological properties and projections. J. Neurosci. *32*, 15076–15085.

Hong, S., Jhou, T.C., Smith, M., Saleem, K.S., and Hikosaka, O. (2011). Negative reward signals from the lateral habenula to dopamine neurons are mediated by rostromedial tegmental nucleus in primates. J. Neurosci. *31*, 11457–11471.

Ilango, A., Kesner, A.J., Keller, K.L., Stuber, G.D., Bonci, A., and Ikemoto, S. (2014). Similar roles of substantia nigra and ventral tegmental dopamine neurons in reward and aversion. J. Neurosci. *34*, 817–822.

Jhou, T.C., Good, C.H., Rowley, C.S., Xu, S.-P., Wang, H., Burnham, N.W., Hoffman, A.F., Lupica, C.R., and Ikemoto, S. (2013). Cocaine drives aversive conditioning via delayed activation of dopamine-responsive habenular and midbrain pathways. J. Neurosci. *33*, 7501–7512.

Johnson, S.W., and North, R.A. (1992). Two types of neurone in the rat ventral tegmental area and their synaptic inputs. J. Physiol. *450*, 455–468.

Kim, T.I., McCall, J.G., Jung, Y.H., Huang, X., Siuda, E.R., Li, Y., Song, J., Song, Y.M., Pao, H.A., Kim, R.-H., et al. (2013). Injectable, cellular-scale optoelectronics with applications for wireless optogenetics. Science *340*, 211–216.

Korotkova, T.M., Ponomarenko, A.A., Brown, R.E., and Haas, H.L. (2004). Functional diversity of ventral midbrain dopamine and GABAergic neurons. Mol. Neurobiol. *29*, 243–259.

Lammel, S., Hetzel, A., Häckel, O., Jones, I., Liss, B., and Roeper, J. (2008). Unique properties of mesoprefrontal neurons within a dual mesocorticolimbic dopamine system. Neuron *57*, 760–773.

Lammel, S., Ion, D.I., Roeper, J., and Malenka, R.C. (2011). Projection-specific modulation of dopamine neuron synapses by aversive and rewarding stimuli. Neuron *70*, 855–862.

Lammel, S., Lim, B.K., Ran, C., Huang, K.W., Betley, M.J., Tye, K.M., Deisseroth, K., and Malenka, R.C. (2012). Input-specific control of reward and aversion in the ventral tegmental area. Nature *491*, 212–217.

Lammel, S., Lim, B.K., and Malenka, R.C. (2014). Reward and aversion in a heterogeneous midbrain dopamine system. Neuropharmacology *76* (Pt B), 351–359.

Li, W., Doyon, W.M., and Dani, J.A. (2012). Quantitative unit classification of ventral tegmental area neurons in vivo. J. Neurophysiol. *107*, 2808–2820.

Li, X., Qi, J., Yamaguchi, T., Wang, H.-L., and Morales, M. (2013). Heterogeneous composition of dopamine neurons of the rat A10 region: molecular evidence for diverse signaling properties. Brain Struct. Funct. *218*, 1159–1176.

Lindeberg, J., Usoskin, D., Bengtsson, H., Gustafsson, A., Kylberg, A., Söderström, S., and Ebendal, T. (2004). Transgenic expression of Cre recombinase from the tyrosine hydroxylase locus. Genesis *40*, 67–73.

Margolis, E.B., Toy, B., Himmels, P., Morales, M., and Fields, H.L. (2012). Identification of rat ventral tegmental area GABAergic neurons. PLoS ONE *7*, e42365.

Matsumoto, M., and Hikosaka, O. (2007). Lateral habenula as a source of negative reward signals in dopamine neurons. Nature *447*, 1111–1115.

Matsumoto, M., and Hikosaka, O. (2009). Representation of negative motivational value in the primate lateral habenula. Nat. Neurosci. *12*, 77–84.

Meye, F.J., Lecca, S., Valentinova, K., and Mameli, M. (2013). Synaptic and cellular profile of neurons in the lateral habenula. Front. Hum. Neurosci. *7*, 860.

Min, N., Joh, T.H., Kim, K.S., Peng, C., and Son, J.H. (1994). 5′ upstream DNA sequence of the rat tyrosine hydroxylase gene directs high-level and tissue-specific expression to catecholaminergic neurons in the central nervous system of transgenic mice. Brain Res. Mol. Brain Res. *27*, 281–289.

Nair-Roberts, R.G., Chatelain-Badie, S.D., Benson, E., White-Cooper, H., Bolam, J.P., and Ungless, M.A. (2008). Stereological estimates of dopaminergic, GABAergic and glutamatergic neurons in the ventral tegmental area, substantia nigra and retrorubral field in the rat. Neuroscience *152*, 1024–1031.

Olson, V.G., and Nestler, E.J. (2007). Topographical organization of GABAergic neurons within the ventral tegmental area of the rat. Synapse *61*, 87–95.

Roeper, J. (2013). Dissecting the diversity of midbrain dopamine neurons. Trends Neurosci. *36*, 336–342.

Root, D.H., Mejias-Aponte, C.A., Zhang, S., Wang, H.-L., Hoffman, A.F., Lupica, C.R., and Morales, M. (2014a). Single rodent mesohabenular axons release glutamate and GABA. Nat. Neurosci. *17*, 1543–1551.

Root, D.H., Mejias-Aponte, C.A., Qi, J., and Morales, M. (2014b). Role of glutamatergic projections from ventral tegmental area to lateral habenula in aversive conditioning. J. Neurosci. *34*, 13906–13910.

Rothermel, M., Brunert, D., Zabawa, C., Díaz-Quesada, M., and Wachowiak, M. (2013). Transgene expression in target-defined neuron populations mediated by retrograde infection with adeno-associated viral vectors. J. Neurosci. *33*, 15195–15206.

Savitt, J.M., Jang, S.S., Mu, W., Dawson, V.L., and Dawson, T.M. (2005). Bcl-x is required for proper development of the mouse substantia nigra. J. Neurosci. *25*, 6721–6728.

Sawamoto, K., Nakao, N., Kobayashi, K., Matsushita, N., Takahashi, H., Kakishita, K., Yamamoto, A., Yoshizaki, T., Terashima, T., Murakami, F., et al. (2001). Visualization, direct isolation, and transplantation of midbrain dopaminergic neurons. Proc. Natl. Acad. Sci. USA *98*, 6423–6428.

Shabel, S.J., Proulx, C.D., Trias, A., Murphy, R.T., and Malinow, R. (2012). Input to the lateral habenula from the basal ganglia is excitatory, aversive, and suppressed by serotonin. Neuron *74*, 475–481.

Skagerberg, G., Lindvall, O., and Björklund, A. (1984). Origin, course and termination of the mesohabenular dopamine pathway in the rat. Brain Res. *307*, 99–108.

Stamatakis, A.M., and Stuber, G.D. (2012). Activation of lateral habenula inputs to the ventral midbrain promotes behavioral avoidance. Nat. Neurosci. *15*, 1105–1107.

Stamatakis, A.M., Jennings, J.H., Ung, R.L., Blair, G.A., Weinberg, R.J., Neve, R.L., Boyce, F., Mattis, J., Ramakrishnan, C., Deisseroth, K., and Stuber, G.D. (2013). A unique population of ventral tegmental area neurons inhibits the lateral habenula to promote reward. Neuron *80*, 1039–1053.

Steinberg, E.E., Keiflin, R., Boivin, J.R., Witten, I.B., Deisseroth, K., and Janak, P.H. (2013). A causal link between prediction errors, dopamine neurons and learning. Nat. Neurosci. *16*, 966–973.

Stuber, G.D., Stamatakis, A.M., and Kantak, P.A. (2015). Considerations when using Cre-driver rodent lines for studying ventral tegmental area circuitry. Neuron *85*, 439–445.

Swanson, L.W. (1982). The projections of the ventral tegmental area and adjacent regions: a combined fluorescent retrograde tracer and immunofluorescence study in the rat. Brain Res. Bull. *9*, 321–353.

Tan, K.R., Yvon, C., Turiault, M., Mirzabekov, J.J., Doehner, J., Labouèbe, G., Deisseroth, K., Tye, K.M., and Lüscher, C. (2012). GABA neurons of the VTA drive conditioned place aversion. Neuron *73*, 1173–1183.

Tsai, H.C., Zhang, F., Adamantidis, A., Stuber, G.D., Bonci, A., de Lecea, L., and Deisseroth, K. (2009). Phasic firing in dopaminergic neurons is sufficient for behavioral conditioning. Science *324*, 1080–1084.

Tye, K.M., Mirzabekov, J.J., Warden, M.R., Ferenczi, E.A., Tsai, H.-C., Finkelstein, J., Kim, S.-Y., Adhikari, A., Thompson, K.R., Andalman, A.S., et al. (2013). Dopamine neurons modulate neural encoding and expression of depression-related behaviour. Nature *493*, 537–541.

Ungless, M.A., and Grace, A.A. (2012). Are you or aren't you? Challenges associated with physiologically identifying dopamine neurons. Trends Neurosci. *35*, 422–430.

Walsh, J.J., Friedman, A.K., Sun, H., Heller, E.A., Ku, S.M., Juarez, B., Burnham, V.L., Mazei-Robison, M.S., Ferguson, D., Golden, S.A., et al. (2014). Stress and CRF gate neural activation of BDNF in the mesolimbic reward pathway. Nat. Neurosci. *17*, 27–29.

Yizhar, O., Fenno, L.E., Davidson, T.J., Mogri, M., and Deisseroth, K. (2011). Optogenetics in neural systems. Neuron *71*, 9–34.

Zhuang, X., Masson, J., Gingrich, J.A., Rayport, S., and Hen, R. (2005). Targeted gene expression in dopamine and serotonin neurons of the mouse brain. J. Neurosci. Methods *143*, 27–32.